J Therm Anal Calorim (2010) 101:1161–1165
DOI 10.1007/s10973-009-0556-8

Study of the MS response by TG–MS in an acid mine drainage efflorescence

A. Alcolea · I. Ibarra · A. Caparrós · R. Rodríguez

Received: 2 September 2009 / Accepted: 9 October 2009 / Published online: 4 November 2009

Abstract The aim of this study is to employ a thermogravimetric analyzer coupled to a mass spectrometer to research into the influence of heating rate and sample mass on the response of the detector. That response is examined by means of a particular efflorescence taken from an acid mine drainage environment. This mixture of weathered products is mainly composed by secondary sulfate minerals, which are formed in evaporation conditions, appearing as efflorescence salts. Thermogravimetry coupled to mass spectrometry has been used to analyze the three main loss steps that happen when this combination of minerals is heated from 30 to 1,100 °C. This inorganic material is based on a mixture of hexahydrite, zinc sulfate hexahydrate, apjonite, gypsum, plumbojarosite, calcite, quartz, and magnetite. While heating, three main effluent gases evolved from this efflorescence. At a standard heating rate of 10 °C/min, loss of water (dehydration) occurred over 30–500 °C in four major steps, loss of carbon dioxide (decarbonisation) occurred over 200–800 °C in three steps, and loss of sulfur trioxide (desulfation) occurred over 400–1,100 °C in three steps. According to the results, thermal analysis is an excellent technique for the study of decomposition in these systems.

A. Alcolea (✉) · I. Ibarra · A. Caparrós
Servicio de Apoyo a la Investigación Tecnológica, Universidad Politécnica de Cartagena, 30202 Cartagena, Murcia, Spain
e-mail: alberto.alcolea@sait.upct.es

R. Rodríguez
Instituto Geológico y Minero de España, Ríos Rosas, 23, 28003 Madrid, Spain

Keywords Decomposition · Thermogravimetry · Evolved gas analysis · Mass spectrometry · Sulfate minerals

Introduction

Evolved gas analysis (EGA) measures the nature and quantity of volatile products released on heating. In practice, it is often performed simultaneously with thermogravimetry (TG) or thermogravimetry combined with differential scanning calorimetry (TG–DSC), and is particularly useful in supplying direct chemical information to complement the physical data obtained from TG or DSC. Additional advantages that have emerged include specificity—a single decomposition can be followed against a background of concurrent processes—and sensitivity, which can be far greater than with TG alone. EGA is of great value in the interpretation of complex TG and DSC curves.

Regarding to instrumentation, almost every imaginable type of gas detector or analyzer has been utilized in EGA, including hygrometers, nondispersive infrared analyzers, and gas chromatographs. Absorption of the products into solution permits analysis by coulometry, colorimetry, ion selective electrode measurements, or titrimetry. The most important analyzers are Fourier transform infrared (FTIR) spectrometers and, preeminently, mass spectrometers (MS). The two latter methods can be used to record spectra repetitively, thereby producing a time-dependent record of the composition of the gas phase, from which EGA curves can be constructed for selected species [1–4].

Time is the common parameter that makes possible the combination between the TG and the detector. An interpretation of a measurement first of all requires a detailed study of the TG curve. In addition to the quantification of

the mass loss steps, the DTG curve, that is, the first derivative of the TG curve, allows the data obtained from the TG to be correlated with that from the spectrometer. When the sample undergoes a change in mass, a peak minimum in the DTG curve (maximum rate of change mass) should correspond closely to a maximum in the signal intensity curve measured by the gas analyzer. Ideally a detector has the support of vapor phase spectral databases.

In the MS typically used for hyphenated techniques, sample molecules enter the system through an ion source compartment where they are bombarded with a beam of high-energy electrons (usually about 70 eV). This energy is greater than the ionization potentials and bond strength of most molecules. It is in fact sufficient to remove one or more electrons from molecules to form positively charged molecular ions. The excess energy also causes fragmentation of the molecules. This is the reason why it is followed an m/z value of 64 (SO_2^+), although SO_3 is the gas evolved from the sample. The measurement mode used in this article was multiple ion detection (MID), method with which it is possible scan only a selected number of ions, in this article, 18, 44, and 64. The dwell time that the analyzer remains at a given m/z value can be thereby greatly increased longer than in a full scanning method, what improves its sensitivity [5–11].

Thermal analysis is widely used in the study of minerals, for its identification, quantitative analysis, isomorphism transitions, existence of certain molecules, or ions, etc. Sulfate and silicate minerals can bear free, crystalline, and constitution water. These kinds of specimens, while heating, can undergo dehydration, decomposition, polymorphic transformation, recrystallization, melting, and valence-state change of variable-valence elements [12]. Other helpful techniques used to examine these types of samples include vibrational spectroscopy (Raman and infrared), X-ray spectroscopy (by energy dispersion in a scanning electron microscope or by wavelength dispersion in an X-ray fluorescence spectrometer), and X-ray diffraction (XRD) [13–15].

Experimental

Location

The sample object of this study was collected in the spot called "Gravimetría II, 2ª Paz," a gravity concentration spoil deposit located in Cartagena municipality (Region of Murcia, Southeast of Spain), U.T.M. coordinates (x, y) = (690672, 4165545), in the surroundings of the village called "El Llano del Beal." This efflorescence was found on a very steep slope in the tailings area. Location is shown in Fig. 1a and observation under stereomicroscope at 40× magnification is shown in Fig. 1b.

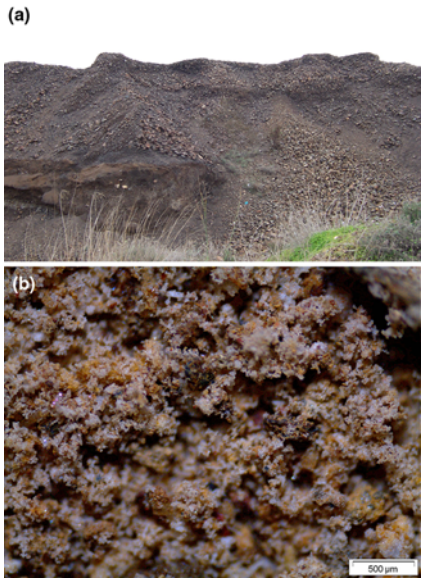

Fig. 1 **a** Sampling location and **b** stereomicroscope observation

Mineralogy

Sample was analyzed by XRD for phase identification and by wavelength dispersive X-ray fluorescence spectrometry (XRF) for quantitative elemental analysis. By XRD were mainly found sulfates (hexahydrite, zinc sulfate hexahydrate, apjonite, gypsum, plumbojarosite), oxides (quartz, magnetite), and silicates (clinochlore). By XRF was found the next composition: 0.29% of Na, 3.37% of Mg, 2.27% of Al, 9.44% of Si, 270 ppm of P, 6.09% of S, 845 ppm of Cl, 0.15% of K, 1.17% of Ca, 0.11% of Ti, 62 ppm of Cr, 1.48% of Mn, 23.28% of Fe, 25 ppm of Co, 41 ppm of Ni, 236 ppm of Cu, 1.66% of Zn, 708 ppm of As, 28 ppm of Rb, 29 ppm of Sr, 27 ppm of Zr, 89 ppm of Cd, 88 ppm of Sb, and 2.47% of Pb. These proportions reveal that such mineral systems can act as a significant heavy metal environmental sink [16–26].

Thermal analysis

After sampling, the specimen was placed immediately in a plastic bag and sealed for shipment to the laboratory. Afterward, the sample was dried at 60 °C for 24 h (in order to release most of the free water) and ground in a disc mill for 1 min until a final particle size lesser than 40 µm. Although it is possible to separate the sulfate minerals by hand, picking up the crystals under the stereomicroscope, it was preferred to study the sample as it occurred in the tailings dump, without any other manipulation.

Thermal decomposition of the samples was performed in a TGA/DSC 1 HT thermogravimetric analyzer (Mettler-Toledo GmbH, Schwerzenbach, Switzerland) with a

flowing nitrogen atmosphere (70 mL/min). Program temperature ranged from 30 to 1,100 °C. All of the TG measurements were blank curve corrected, and alumina pans of 70 μL capacity, without lid, were used. The TG instrument was coupled to a Balzers Thermostar mass spectrometer (Pfeiffer Vacuum, Asslar, Germany) for gas analysis. Only water vapor, carbon dioxide, and sulfur dioxide were analyzed. Dwell time for every ion was 1 s and cathode voltage in the ion source was 65 V. Quadrupole mass spectrometer model was QMS 200 M3.

In order to evaluate the MS response, two different sequences of experiments were carried out. The first study dealt with the influence of the heating rate on MS response. Heating rates of 5, 10, 20, 30, 40, and 50 °C/min and sample mass of approximately 10 mg were used. The second study discussed the influence of sample mass on MS sensitivity. Sample masses close to 0.1, 0.5, 1, 3, and 10 mg and a heating rate of 30 °C/min were used.

Results and discussion

Thermogravimetric analysis and mass spectrometric analysis

The thermal analysis of the sample is shown in Fig. 2. This figure shows a thermogravimetric curve and the differential thermogravimetric curve for the efflorescence. It was performed with standard conditions, that is, 10 mg of sample and a heating rate of 10 °C/min. Due to the complexity of the mixture, this curve shows a permanent mass loss over the entire temperature range. A succession of five main mass loss steps is observed at 104, 109, 252, 495, and 824 °C. The extension and number of these steps depend on the types and proportion of the different mineral species involved in the sample [27–32].

The ion current curve for evolved gases is shown in Fig. 3. This figure shows that water vapor is the evolved gas from 30 to 500 °C, carbon dioxide occurred over 200–800 °C, and loss of sulfur trioxide occurred over 400–1100 °C. The addition of the MS curves follows the DTG curve precisely. As there are different crystal structures involved in the decomposition process, superimposition of evolved gases makes impossible assign every step to a single chemical reaction. It can be estimated that the mass loss of water was 10%, the mass loss of carbon dioxide was 2%, and the mass loss of sulfur trioxide was 15%.

Influence of the heating rate on mass spectrometer response

Samples of this efflorescence were decomposed with TG at heating rates of 5, 10, 20, 30, 40, and 50 °C/min and the corresponding signals were recorded. The curves exhibit several mass loss steps that shift toward higher temperatures with increasing heating rates.

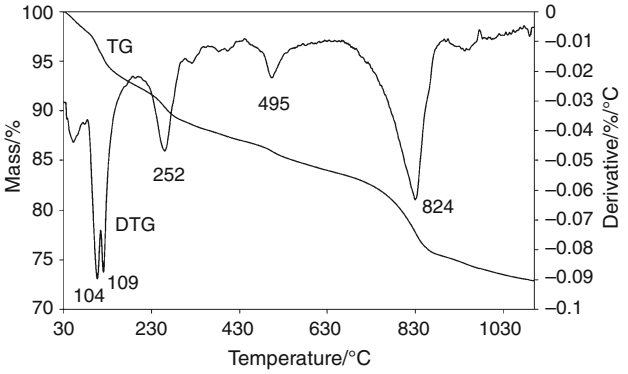

Fig. 2 TG and DTG curves of the efflorescence

Mass spectrometer curves show that decomposition process depends on the heating rates; higher heating rates shift the onset of decomposition and the decomposition range of every ion mass to higher temperatures.

The *m*/*z* 18, 44, and 64 ion curves were measured at each different heating rate, and the corresponding peak areas were computed. The results are summarized in Table 1. The TG curves showed that the mass losses were the same for each sample, that is, the amount of gasses evolved was independent of the heating rate. Constant peaks areas for the *m*/*z* 18, 44, and 64 curves were, therefore, also expected. In fact the evaluated peak area, normalized to sample size, shows a slight increase at higher heating rates for the *m*/*z* 18 ion, and a slight decrease for the *m*/*z* 44 and 64 ions. Graphical results can be found in Fig. 4.

Influence of sample mass on mass spectrometer sensitivity

Sample masses of approximately 0.1, 0.5, 1, 3, and 10 mg were decomposed with TG at a temperature change rate of

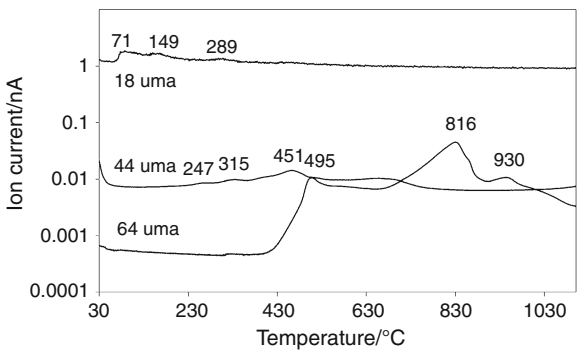

Fig. 3 Ion current of evolved gases for the decomposition of the sample

Table 1 Integration of ion curves in evolved gases for the decomposition of the efflorescence

Heating rate/°C/min	Size/mg	MS peak area/nsA			Normalized MS peak area/nsA/mg		
		m/z 18	*m/z* 44	*m/z* 64	*m/z* 18	*m/z* 44	*m/z* 64
5	9.9229	225.74	11.84	60.54	22.75	1.19	6.10
10	9.7807	591.12	10.52	47.33	60.44	1.08	4.84
20	10.4176	619.64	9.87	47.17	59.48	0.95	4.53
30	9.9231	648.84	8.83	42.41	65.39	0.89	4.27
40	9.6917	658.35	8.25	39.52	67.93	0.85	4.08
50	9.5591	668.95	7.61	37.34	69.98	0.80	3.91

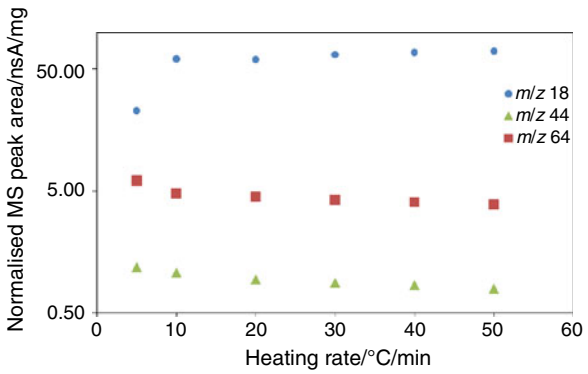

Fig. 4 Normalised peak area as a function of heating rate for the *m/z* values 18, 44, and 64

Table 2 Evaluation of the MS peak areas for *m/z* 18, 44, and 64

Mass/mg	MS peak area/nsA		
	m/z 18	*m/z* 44	*m/z* 64
0.1622	333.90	0.04	0.61
0.3952	337.52	0.34	1.90
0.8995	357.51	0.99	4.32
2.9411	364.24	2.49	11.06
9.9231	676.12	8.86	42.39

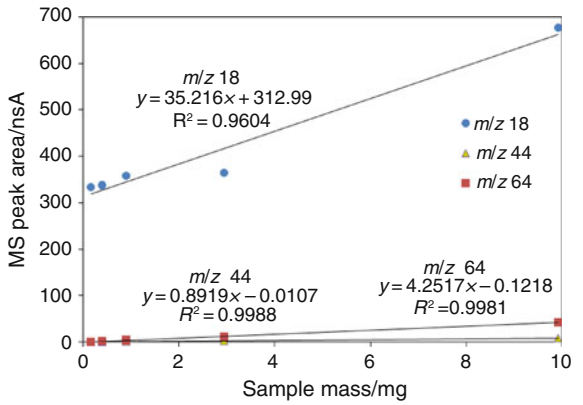

Fig. 5 Peak area as a function of sample mass for the *m/z* values 18, 44, and 64

30 °C/min. This value of heating rate was chosen due to its centrality in the previous study. The recorded curves exhibit several mass loss steps that do not shift toward higher temperatures with increasing sample size in a substantial fashion.

Mass spectrometer measurements show that peak heights and peak areas of water, carbon dioxide, and sulfur trioxide are directly proportional to the sample masses used. These correlations are summarized in Table 2 and displayed in Fig. 5.

The TG curves showed that the mass loss percentages for the decomposition were the same for each sample.

Conclusions

Thermogravimetric analysis coupled to an MS has been used to study the thermal decomposition of an efflorescent salt original from Southeast of Spain. This mineral consists of a mixture of sulfates, silicates, and oxides, formed in an acid mine drainage environment. The specimen shows a wide temperature range from 30 to 500 °C for water loss, a temperature range over 200–800 °C for carbon dioxide loss, and a temperature range over 400–1,100 °C for sulfur trioxide loss. Although there is a continuous mass loss over the entire temperature range, DTG and MS curves reveal that mass loss steps associated with dehydroxylation are 47, 71, 104, 109, 149, and 289 °C; mass loss steps attributed to carbon dioxide are 247, 315, 366, 387, 451, and 656 °C and, finally, mass loss steps related to sulfur trioxide are 495, 816, and 930 °C.

Regarding to the influence of the heating rate on MS response, although only a slight dependence was found, it is clear that low heating rates (5 °C/min) give a poorer spectrometric response for a *m/z* value of 18. This is the reason why choosing a heating rate of 15–30 °C/min is a good compromise between resolution and productivity for all the *m/z* values of interest.

The measurements on the decomposition of the efflorescence demonstrate the linear relationship between MS

peak area and sample mass. This can be used to calibrate and adjust the MS signal, regarding every *m*/*z* value.

It is worth emphasizing the different performance of the MS with *m*/*z* 18, for which correlations are not so good. The high baseline level for this ion is related to the adsorption of water on the surface of the vacuum chamber in mass spectrometer and could possibly be lowered with a baking process of the vacuum chamber for 3 h and letting an inert gas flows for the next 24 h, previously to running the samples. In this way, correlation for this ion could be improved, by decreasing the ion current in a decade factor.

Acknowledgements The authors wish to thank and gratefully acknowledge the infrastructure support of the Assistance Service for Technological Research in Technical University of Cartagena (Spain).

References

1. Warrington SB. Thermal analysis and calorimetry. In: Günzler H, Williams A, editors. Handbook of analytical techniques. Weinheim, Germany: Wiley-VCH Verlag GmbH; 2001. p. 833–4.
2. Lodding W, editor. Gas effluent analysis. New York: Marcel Dekker; 1967.
3. Warrington SB. Evolved gas analysis. In: Charsley EL, Warrington SB, editors. Thermal analysis—techniques and applications. London: Royal Society of Chemistry; 1992.
4. Holdiness MR. Evolved gas analysis by mass spectrometry: a review. Thermochim Acta 1984;75:361.
5. Mettler-Toledo GmbH. Evolved gas analysis. 2001. p. 4–7, 27–29, 37–38.
6. McLafferty FW, Turecek F. Interpretation of mass spectra. 4th ed. Mill Valley, CA: University Science Books; 1993.
7. Busch KL, Lehman TA. Guide to mass spectrometry. Weinheim: VCH Verlagsgesellschaft GmbH; 1996.
8. de Hoffmann E, Charette J, Stroobant V. Mass spectrometry: principles and applications. Chichester: Wiley; 1996.
9. Watson JTh. Introduction to mass spectrometry. 3rd ed. Philadelphia, PA: Lippincott-Raven; 1997.
10. Lee TA. A beginner's guide to mass spectral interpretation. Chichester, England: Wiley; 1998.
11. Smith RM, Busch KL. Understanding mass spectra—a basic approach. New York: Wiley; 1999.
12. Hatakeyama T, Liu Z. Thermal analysis curves of minerals. In: Hatakeyama T, Liu Z, editors. Handbook of thermal analysis. Chichester, England: Wiley; 1998. p. 247–336.
13. Frost RL, Weier M, Martinez-Frias J, Rull F, Reddy BJ. Sulphate efflorescent minerals from El Jaroso Ravine, Sierra Almagrera—an SEM and Raman spectroscopic study. Spectrochim Acta 2007;66A:177–183.
14. Frost RL, Weier ML, Kloprogge JT, Rull F, Martinez-Frias J. Raman spectroscopy of halotrichite from Jaroso, Spain. Spectrochim Acta 2005;62A:176–180.
15. Joeckel RM, Ang Clement BJ, VanFleet Bates LR. Sulfate-mineral crusts from pyrite weathering and acid rock drainage in the Dakota Formation and Graneros Shale, Jefferson County, Nebraska. Chem Geol 2005;215:433–452.
16. Hammarstrom JM, Smith KS. Geochemical and mineralogic characterization of solids and their effects on waters in metal-mining environments. U.S. Geological Survey Open-File Report 02-195; 2002.
17. Alpers CN, Blowes DW, Nordstrom DK, Jambor JL. Secondary minerals and acid mine-water chemistry. In: Jambor JL, Blowes DW, editors. The environmental geochemistry of sulfide minewastes. Short course handbook. Waterloo, ON: Mineralogical Association of Canada; 1994. vol. 22, p. 247–70.
18. Baedecker PA, editor. Methods for geochemical analysis. Geological Survey Bulletin; 1987. vol. 1770.
19. Bigham JM. Mineralogy of ochre deposits formed by sulfide oxidation. In: Jambor JL, Blowes DW, editors. The environmental geochemistry of sulfide mine-wastes. Short course handbook. Waterloo, ON: Mineralogical Association of Canada; 1994. vol. 22, p. 103–32.
20. Crock JG, Arbogast BF, Lamothe PJ. Laboratory methods for analysis of environmental samples. In: Plumlee GS, Logsdon MJ, editors. The environmental geochemistry of mineral deposits, part A: processes, techniques, and health issues. Reviews in economic geology. Society of Economic Geologists, Inc. 1999. vol. 6A, p. 265–87.
21. International Centre for Diffraction Data. Powder diffraction file sets 1-47;1997.
22. Jambor JL. Mineralogy of sulfide-rich tailings and their oxidation products. In: Jambor JL, Blowes DW, editors. The environmental geochemistry of sulfide mine-wastes. Short course handbook. Waterloo, ON: Mineralogical Association of Canada; 1994. vol. 22, p. 103–32.
23. Mee JS, Siems DF, Taggart JE Jr. Major element analysis by wavelength dispersive X-ray fluorescence spectrometry. In: Arbogast BF, editor. Analytical methods manual for the Mineral Resource Surveys Program, U.S. Geological Survey: U.S. Geological Survey Open-File Report 96-525; 1996. p. 237–42.
24. MEND. Review of waste rock sampling techniques. Mine Environement Neutral Drainage (MEND) Program Report 4.5.1. Prepared by SENES Consultants Ltd., Golder Associee Ltee, and Laval University; 1994.
25. Sobek AA, Schuller WA, Freeman JR, Smith RM. Field and laboratory methods applicable to overburden and minesoils: EPA 600/2-78-054. 1978. 203 pp.
26. Taggart JE Jr, Lindsay JR, Scott BA, Vivit DV, Bartel AJ, Stewart KC. Analysis of geologic materials by wavelength-dispersive X-ray fluorescence spectrometry. In: Baedecker PA, editor. Methods for geochemical analysis. U.S. Geological Survey Bulletin. 1987. vol. 1770, p. E1–19.
27. Frost RL, Weier ML, Martens W. Thermal decomposition of jarosites of potassium, sodium and lead. J Therm Anal Calorim. 2005;82:115–8.
28. Frost RL, Wills R-A, Kloprogge JT, Martens W. Thermal decomposition of ammonium jarosite $(NH_4)Fe_3(SO_4)_2(OH)_6$. J Therm Anal Calorim. 2006;84:489–96.
29. Frost RL, Wills R-A, Kloprogge JT, Martens WN. Thermal decomposition of hydronium jarosite $(H_3O)Fe_3(SO_4)2(OH)_6$. J Therm Anal Calorim. 2006;83:213–8.
30. Locke AJ, Martens WN, Frost RL. Thermal analysis of halotrichites. Thermochim Acta 2007;459:64–72.
31. Thomas PS, Hirschausen D, White RE, Guerbois JP, Ray AS. Characterisation of the oxidation products of pyrite by thermogravimetric and evolved gas analysis. J Therm Anal Cal. 2003;72:769.
32. Drouet C, Navrotsky A. Synthesis, characterization, and thermochemistry of K-Na-H3O jarosites. Geochim Cosmochim Acta. 2003;67:2063.